



Research article

Long non-coding RNA LINC01554 overexpression suppresses viability, migration, and invasion of liver cancer cells through regulating miR-148b-3p/EIF4E3

Xiaojing Ren^{a,b}, Xiaoxiao Wang^b, Huangqin Song^b, Chao Zhang^b, Junlong Yuan^b, Jiefeng He^{b,**}, Jianguo Li^{a,***}, Zhuangqiang Wang^{b,*}

^a Radiological & Environment Medicine Dept, China Institute for Radiation Protection, Taiyuan, 030032, China

^b Department of Hepatobiliary Surgery, Shanxi Bethune Hospital, Shanxi Academy of Medical Sciences, Tongji Shanxi Hospital, Third Hospital of Shanxi Medical University, Taiyuan, 030032, China

ARTICLE INFO

Keywords:

Liver cancer
LINC01554
miR-148b-3p
EIF4E3
ceRNA

ABSTRACT

Background: Long non-coding RNAs (lncRNAs) can be severed as competing endogenous RNAs (ceRNAs) to regulate target genes or mRNAs via sponging microRNAs (miRNAs). This study explored the effect of LINC01554 on liver cancer cells through the ceRNA mechanism.

Methods: Five significantly down-regulated lncRNAs were selected for further verification, and then through bioinformatics, interactive miRNAs and mRNAs of lncRNAs were identified. The relationship between LINC01554, miR-148b-3p and EIF4E3 was detected by the dual luciferase reporter gene assay. Afterwards, HCCLM3 cells were transfected with pCDH-LINC01554, miR-148b-3p inhibitor and miR-148b-3p mimics. Cell viability, apoptosis, migration and invasion were measured by Cell Counting Kit-8, flow cytometer, and Transwell assays. Real-time quantitative PCR (RT-qPCR) and Western blot were used to measure the expressions of related genes and proteins.

Results: LINC01554 was significantly down-regulated in the liver cancer cell lines, and was expressed in the cytoplasm of HCCLM3 cells. LINC01554 overexpression inhibited proliferation, migration, and invasion of HCCLM3 cells, and promote their apoptosis ($P < 0.05$). Besides, LINC01554 overexpression also significantly increased the levels of *BAX*, *BCL2/BAX*, *P53*, cleaved-*Caspase3*, *TIMP3*, *E-cadherin* and *EIF4E3* ($P < 0.05$). Through bioinformatics and dual-luciferase reporter gene assay, LINC01554, miR-148b-3p and EIF4E3 were proved to interact with each other. Furthermore, the effects of miR-148b-3p knockdown on HCCLM3 cells were similar with those of LINC01554 overexpression, and miR-148b-3p mimics could reverse the changes of cell viability, apoptosis, migration, and invasion induced by LINC01554 overexpression.

Conclusions: LINC01554 overexpression could suppress the growth and metastasis of HCCLM3 cells via miR-148b-3p/EIF4E3.

* Corresponding author. Department of Hepatobiliary Surgery, Shanxi Bethune Hospital, Shanxi Academy of Medical Sciences, Tongji Shanxi Hospital, Third Hospital of Shanxi Medical University, 99 Longcheng Street, Xiaodian District, Taiyuan, 030032, China.

** Corresponding author. Department of Hepatobiliary Surgery, Shanxi Bethune Hospital, Shanxi Academy of Medical Sciences, Tongji Shanxi Hospital, Third Hospital of Shanxi Medical University, 99 Longcheng Street, Xiaodian District, Taiyuan, 030032, China.

*** Corresponding author. Radiological & Environment Medicine Dept, China Institute for Radiation Protection, 102 Xuefu Street, Xiaodian District, Taiyuan, 030032, China.

E-mail addresses: hejiefeng2008@163.com, jfhe@sxmu.edu.cn (J. He), LJG2547@163.com (J. Li), zhuangqiangwang@126.com (Z. Wang).

<https://doi.org/10.1016/j.heliyon.2024.e27319>

Received 5 September 2023; Received in revised form 27 February 2024; Accepted 27 February 2024

Available online 5 March 2024

2405-8440/© 2024 The Authors. Published by Elsevier Ltd. This is an open access article under the CC BY-NC license (<http://creativecommons.org/licenses/by-nc/4.0/>).

1. Introduction

Liver cancer is the second leading cause of cancer-related deaths worldwide, and its incidence is among the top 5 tumors and is increasing year by year [1]. In 2020, liver cancer had an estimated 0.41 million new cases, and about 0.39 million deaths in China [2]. Etiologically, hepatitis B/C virus infection and alcohol consumption account for more than 80% of liver cancer deaths [3]. Liver cancer has a poor prognosis, and only 5%–15% patients with early liver cancer are suitable for surgical resection [4]. For patients with advanced liver cancer, ablation therapy in combination with chemo therapy is required, but the effects are still not ideal [5]. The overall five-year survival rate for patients with advanced liver cancer is less than 5% [6]. Therefore, in order to improve the prognosis of patients with liver cancer and clarify the mechanisms of the occurrence and development of liver cancer, it is necessary to find the key regulators of liver cancer.

Long noncoding RNAs (lncRNAs) are a group of non-coding RNAs larger than 200 nt [7], and have attracted more and more attentions of researchers. In many cases, lncRNAs have been proved to be primary regulators of gene expressions, therefore, they play key roles in a variety of biological functions and disease development, including cancers [8]. A growing number of researches have demonstrated that lncRNAs can regulate the proliferation, metastasis, invasion and apoptosis of tumor cells [9]. Yuan et al. [10] indicated that lncRNA TLNC1 was identified as the potential tumorigenic lncRNA of liver cancer, and could enhance the growth and metastasis of liver cancer cells *in vitro* and *in vivo* through interacting TRP and regulating p53. Another study showed that lncRNA HAND2-AS1 was highly expressed in the liver cancer stem cells, and could accelerate the self-renewal of liver cancer stem cells, and drive liver tumorigenesis [11]. Xin et al. [12] showed that Excessive lncR HULC inhibits hepatocellular carcinoma (HCC) autophagy by reducing the expression of PTEN and β -catenin in liver cancer cells by miR-15a. All these reports indicate that lncRNAs have essential roles in the occurrence and progression of liver cancer.

In addition, lncRNAs can be severed as competing endogenous RNAs (ceRNAs) to bind with microRNAs (miRNAs), thus further regulating the expressions of target genes or mRNAs [13]. Nowadays, ceRNA networks have been shown to play important roles in the occurrence and development of many kinds of cancers [14]. Yang et al. [15] demonstrated that down-regulated LINC01133 can inhibit APC expression and *Wnt*/ β -catenin pathway through miR-106a-3p to inhibit the progression and metastasis of gastric cancer. Another study identified lncRNA HOTAIR closely related to breast cancer by analyzing the TCGA database, and further found that lncRNA HOTAIR regulates the expression of HMGA2 through miR-20a-5p, which in turn affects breast cancer progressions [16]. However, so far, only few studies have identified lncRNAs related to liver cancer, and their associated ceRNA mechanisms in liver cancer remain unclear.

In addition, our previous study has showed that 175 differentially expressed lncRNAs (DE-lncRNAs), including 96 up-regulated lncRNAs and 79 down-regulated lncRNAs, were identified to be associated with liver cancer [17]. On this basis, we randomly selected five significantly down-regulated lncRNAs (HAND2-AS1, LINC01554, SOCS2-AS1, LINC00659 and RP11-557H15.4) for further verification. By analyzing and searching for the literatures, the roles of lncRNA HAND2-AS1 in liver cancer have been fully reported previously ([11,18]), while no studies have reported the specific roles of lncRNA RP11-557H15.4 in human diseases. For lncRNA LINC01554, some studies have reported its roles in other cancers, such as NSCLC [19], laryngeal squamous cell carcinoma [20], and esophageal squamous cell carcinoma [21], but its action mechanisms in liver cancer are still unclear. Therefore, LINC01554 was chosen as the target subject in this study, and the effects of LINC01554 on liver cancer cells were explored. Then, the interactive miRNAs and mRNAs of LINC01554 were screened through bioinformatics, and validated in liver cancer cells and liver cancer tissue samples. Finally, the axis of LINC01554, miR-148b-3p and EIF4E3 was chosen to investigate the ceRNA mechanisms in liver cancer. We hypothesized that LINC01554 may be served as a ceRNA to sponge with miR-148b-3p to further regulate EIF4E3 expression, thereby participating in liver cancer progression. These findings will improve our understanding of liver cancer, and provide novel therapeutic targets and pathways for liver cancer.

2. Materials and methods

2.1. Cell culture and patient collection

LX2 cells (cat no. CL-0560) and HCCLM3 cells (cat no. CL-0278) were obtained from Procell Life Science & Technology Co., Ltd. (Wuhan, China), as well as HepG2 cells (cat no. SCSF-510) and PLC/PRF/5 cells (cat no. SCSF-5059) were purchased from Cell bank, Chinese Academy of Sciences (Shanghai, China). Among them, LX2 cells were cultured in Dulbecco's modification of Eagle's medium (DEME, cat no. 11995500BT, Gibco, Grand Island, NY) supplemented with 10% fetal calf serum (FBS, cat no. 10099-141, Gibco) and 1% penicillin/streptomycin (cat no. 15140-122, Gibco); and HCCLM3 cells were cultured in DMEM/F12 (cat no. C11330500BT) with 10% FBS and 1% penicillin/streptomycin. Both HepG2 cells and PLC/PRF/5 cells were cultured in Minimum Essential Medium (MEM, cat no. 41500034, Gibco) contained with 10% FBS and 1% penicillin/streptomycin. All these cell lines were maintained in an incubator with 5% CO₂ at 37 °C. When the cells reached to 80%–90% confluence, the cells were passaged.

Five liver cancer patients aged 64.4 \pm 8.4 years without drug treatment were recruited from Shanxi Dayi Hospital, People's Hospital of Zhengzhou University, and Henan Provincial People's Hospital. The liver cancer diagnosis was based on histological examination, and no distant metastasis was detected. The cancer tissues and paracancerous tissues were obtained from the five patients for further verification. This study was approved by the Ethic Committee of Shanxi Bethune Hospital (Shanxi, China) (approval no. YXLL-2022-005); and written informed consent was obtained from all patients.

2.2. Real-time quantitative PCR (RT-qPCR)

Total RNA was extracted from the cells or tissues using RNAiso Plus (cat no. 9109, Trizol, Takara Biomedical Technology Co., Ltd., Beijing, China) following the manufacturer's instructions. The purity and concentration of the total RNA were determined using a microplate reader. The levels of each miRNA were measured using the stem-loop method, and U6 was served as a reference gene. The total RNA was reversely transcribed into cDNA using PrimeScript™ II 1st Strand cDNA synthesis Kit (cat no. 6210A, Takara Biomedical Technology Co., Ltd.) based on the manufacturer's protocols. The RT-qPCR reaction was initiated at 50 °C for 3min, 95 °C for 3min, followed by a total of 40 cycles at 95 °C for 10s and 60 °C for 30s, and melt curve at 60 °C–95 °C with an increment of 0.5 °C for 10s. Glyceraldehyde-3-phosphate dehydrogenase (GAPDH) was served as a housekeeping gene for lncRNAs and mRNAs. The sequences of all primers were shown in Table 1, and the relative levels of lncRNAs, miRNAs and mRNAs were calculated using the $2^{-\Delta\Delta Ct}$ method

Table 1

The sequences of all primers.

Types	Primer		Sequence (5'-3')
lncRNA	HAND2-AS1	F	TTGGGCGATTTTGAAGTGGC
		R	GTGAGAGGACTGGTTTCGG
	LINC01554	F	GAAGCTGCACACGATGACAC
		R	ACTGCTCATCAACCGACCTC
	SOCS2-AS1	F	GCAGGCAATTTATTGGCAGGC
		R	GCCCCAAATCTGTGCATCTA
	RP11-557H15.4	F	TTCCACCGCTTGATCCCGTA
		R	CTTCTCGTGTCCCGTCACC
	LINC00659	F	GCACCCCTGAAGGACCATATC
		R	CGAGTCACTGAGATGCCCAA
mRNA	ZDHC17	F	GGCCCGGATGAGTACGATAC
		R	TCCAAGAGGTTACCATATCCA
	SLC24A4	F	ATGGCCCCAGTGAATGGGA
		R	CCAGCCACATCTTCGCTCAG
	UBN2	F	GGAGTTCAGTTACCCGGAGC
		R	CGGGGTTTCCACCATATTTTC
	EIF4E3	F	GCAAAGGGTGGCGTATGGAA
		R	CCCGATGGTTGCTAACAGC
	STOX2	F	GACCCGGAGCACAACTTG
		R	GGGAGACATACTGATGGGTGA
	BCL2	F	AGTACTGAACCGGCACCT
		R	CCACCAGGGCCAAACTGAGCA
	BAX	F	CATATAACCCCGTCAACGCAG
		R	GCAGCCGCCACAACATAC
	P53	F	GAGGTGGCTCTGACTGTACC
		R	TCCGTCCAGTAGATTACCAC
	Caspase3	F	CATGGAAGCGAATCAATGGACT
		R	CTGTACCAGACCGAGATGTCA
	E-Cadherin	F	CGAGAGTACACGTTACCGG
		R	GGGTGTCGAGGGAAAATAGG
TIMP3	F	CATGTGCAGTACATCCATACGG	
	R	CATCATAGACGCGACCTGTCA	
GAPDH	F	TGACAACCTTTGGTATCGTGAAGG	
	R	AGGCAGGGATGATGTTCTGGAGAG	
miRNA	miR-2277-5p	F	AGCGCGGGCTGAGCGCTG
		RT	GTCGTATCCAGTGCAGGGTCCGAGGTATTTCGCACTGGATACGACGACTGG
	miR-2682-5p	F	GCGCCAGGCAGTGACTGTTCA
		RT	GTCGTATCCAGTGCAGGGTCCGAGGTATTTCGCACTGGATACGACGACGCTC
	miR-432-5p	F	GTCGTATCCAGTGCAGGGTCCGAGGTATTTCGCACTGGATACGACCCACCC
		RT	GCGCGTCTTGGAGTAGGTCAIT
	miR-4433a-5p	F	GTCGTATCCAGTGCAGGGTCCGAGGTATTTCGCACTGGATACGACATGTCC
		RT	GCGCACAGGAGTGGGGGTG
	miR-148b-3p	F	GCGCTCAGTGCATCACAGAA
		RT	GTCGTATCCAGTGCAGGGTCCGAGGTATTTCGCACTGGATACGACACAAAAG
U6	F	CTCGCTTCGGCAGCACA	
	R	AACGCTTCACGAATTTGCGT	
Cell transfection sequences	Universal downstream primer	RT	GTCGTATCCAGTGCAGGGTCCGAGGTATTTCGCACTGGATACGACAAAATATG
			GTGCAGGGTCCGAGGT
	miR-148b-3p mimics		Sense: UCAGUGCAUCACAGAACUUUGUTT
			Antisense: ACAAAGUUCUGUGAUGCACUGATT
	miR-148b-3p inhibitor		Sense: ACAAAGUUCUGUGAUGCACUGA
			Sense: UUCUCCGACGUGUCACGUTT
	NC mimics		Antisense: ACGUGACACGUUCGGAGAAT
			Sense: CAGUACUUUUGUGUAGUACAA
	NC inhibitor		Antisense: UUGUACUACACAAAAGUACUG

[22].

2.3. Fluorescence in situ hybridization (FISH)

The FISH kit (cat no. C10910, Guangzhou RiboBio Co., Ltd, Guangzhou, China) was used to evaluate the localization of lncRNA LINC01554 in HCCLM3 cells according to the manufacturer's protocols. Briefly, HCCLM3 cells were seeded into a 24-well plate at a density of 6×10^4 cells/well, and cultured to a confluence of 60%–70%. The cells were washed with $1 \times$ PBS for 5 min, and then fixed with 4% paraformaldehyde at room temperature for 10 min. After washing with $1 \times$ PBS for 5 min three times, each well was added 1 mL pre-cooled transparent liquid (PBS containing 0.5% Triton X-100). After incubated at 4 °C for 5 min, the transparent liquid was removed, and the cells were washed with PBS three times. After that, each well was added with prehybridization solution (200 μ L), and blocked at 37 °C for 30 min. After removing the prehybridization solution, 100 μ L hybrid solution containing a probe (2.5 μ L 20 μ M lncRNA LINC01554 FISH probe mix added to 100 μ L hybrid solution, designed by Guangzhou RiboBio Co., Ltd) was added, and then the mixture was incubated in the dark at 37 °C overnight. After washing with hybridization solution I, II, III and PBS, the cells were fixed on slides using DAPI, and the images were taken under a fluorescence microscope (model no. IX70, Olympus Corporation, Japan). After that, total RNA from cell nucleus and cytoplasm were isolated using a Nucleoplasmic fractionation kit (cat no. AM1921, Thermo Fisher Scientific) according to the manufacturer's instructions, and then used for RT-qPCR.

2.4. Cell transfection

The pCDH vector, pCDH-LINC01554, pCDH-EIF4E3, miR-148b-3p inhibitor, miR-148b-3p mimics and miRNA negative control (NC) were prepared and purchased from Yanzai biotechnology (Shanghai) Co. Ltd (Shanghai, China), and the cell transfection was conducted as previously described [23]. The sequences of NC mimics, NC inhibitor, miR-148b-3p mimics and miR-148b-3p inhibitor were shown in Table 1. Briefly, HCCLM3 cells were seeded into a 6-well plate at a density of 5×10^5 , and cultured overnight. On the next day, the medium was changed to serum-free medium, and then the cells were transfected with 3 μ g pCDH vector, 3 μ g pCDH-LINC01554, 3 μ g pCDH-EIF4E3, 100 nM miR-148b-3p inhibitor, and 100 nM miRNA-NC or 20 pM miR-148b-3p mimics using Lipofectamine 3000 (cat no. L3000015, Thermo Fisher Scientific, Waltham, MA, USA) following the manufacturer's protocols. After 6 h of transfection, the medium was changed to complete medium. After cultured for another 48 h, the levels of LINC01554, miR-148b-3p and EIF4E3 were detected using RT-qPCR to assess the cell transfection efficiency. The sequences of LINC01554, miR-148b-3p and EIF4E3 were shown in Table 1.

2.5. Dual-luciferase reporter gene assay

The sequences of LINC01554, miR-148b-3p mimics, and EIF4E3 3'-untranslated region (3'-UTR) were synthesized and provided by Yanzai biotechnology (Shanghai) Co. Ltd. Afterwards, psiCHECK-LINC01554 reporter plasmid (psiCHECK-LINC01554) and the 3'-UTR EIF4E3 report plasmid (pGL3-EIF4E3) were constructed using psiCHECK2 vector (Yanzai biotechnology (Shanghai) Co. Ltd) and pGL3-basic vector (Yanzai biotechnology (Shanghai) Co. Ltd), respectively. After that, the psiCHECK vector (0.3 μ g) or psiCHECK2-LINC01554 (0.3 μ g), and pGL3-basic vector (0.3 μ g) or pGL3-EIF4E3 (0.3 μ g) were co-transfected to 293T cells with miR-148b-3p mimics (100 nM) or negative control (NC) mimics (100 nM) using Lipofectamine 3000 (cat no. L3000015, Thermo Fisher Scientific) in line with the manufacturer's instructions. After cultured for 48 h, the luciferase reactivity was examined using a dual luciferase reporter system (cat no. E1910, Promega, Madison, WI, USA).

2.6. Cell viability and apoptosis

The viability of cells with different treatments was determined using Cell Counting Kit-8 (CCK-8, cat no. C0038, Beyotime Biotechnology, Shanghai, China) based on the manufacturer's instructions. Briefly, the cells were seeded into a 96-well plate at a density of 1×10^4 , and cultured overnight. After transfection, the medium was changed, and cultured for another 24 h, 48 h and 72 h. Each well was added with 10 μ L CCK-8 reagent. After 2 h of incubation, the absorbance at 450 nm was measured using a microplate reader.

After that, cell apoptosis was determined using an Annexin V-FITC/PI apoptosis assay kit (cat no. C1062 M, Beyotime Biotechnology, Shanghai, China) according to the manufacturer's protocols. The cells with different treatments were harvested, and resuspended with PBS. After centrifuged at 1000 g for 5 min, the cells were resuspended with 195 μ L Annexin V-FITC binding solution, and then 5 μ L Annexin V-FITC was added. After that, 10 μ L propidium iodide (PI) was added, and the mixture was incubated in the dark at 25 °C. After 15 min of incubation, a flow cytometer was used to acquire the cells, and the apoptosis rate was calculated by CellQuest software (Becton, Dickinson and Company, NJ, USA).

2.7. Cell migration and invasion

Transwell chambers (pore size 8 μ m; cat no. TCS013024, Guangzhou Jet Bio-Filtration Co., Ltd., Guangzhou, China) were used to evaluate cell migration and invasion. For cell invasion assay, Transwell chambers were previously coated with matrix glue (cat no. 356234, Becton, Dickinson and Company), and then the Transwell chambers coated with matrix glue were put in the pre-cooled 24-well plate for use. The cells with different treatments were collected, and resuspended with serum-free medium at a final density of $5 \times$

10^5 . The cells were inoculated to the upper insert of Transwell chambers, and the lower chamber of Transwell chambers was the complete medium. After 48 h of incubation, the cells were fixed with 4% paraformaldehyde for 20 min. After washing with PBS three times, the cells were stained with crystal violet (cat no. C0121, Beyotime Biotechnology) at room temperature for 20 min. After washing and removing the excess dye, the stained cells were observed under a microscope at a magnification of $100\times$.

2.8. Colony formation

The cells with different treatment were obtained, and were seeded to a 6-well plate at a density of 250 cells/well. After incubated for 14 d, the cells were harvested and rinsed with PBS. The cells were then fixed with 4% paraformaldehyde for 20 min. After washing with PBS twice, crystal violet was added to stain the cells. After incubated at room temperature for 20 min, the cells were washed with PBS. The images were taken under a microscope, and the colony counts were counted.

2.9. Western blot

Total proteins were extracted from the cells with different treatments using RIPA lysis buffer (cat no. P0013B, Beyotime Biotechnology), and the concentrations of the total proteins were determined using a BCA assay kit (cat no. AR0146, Boster

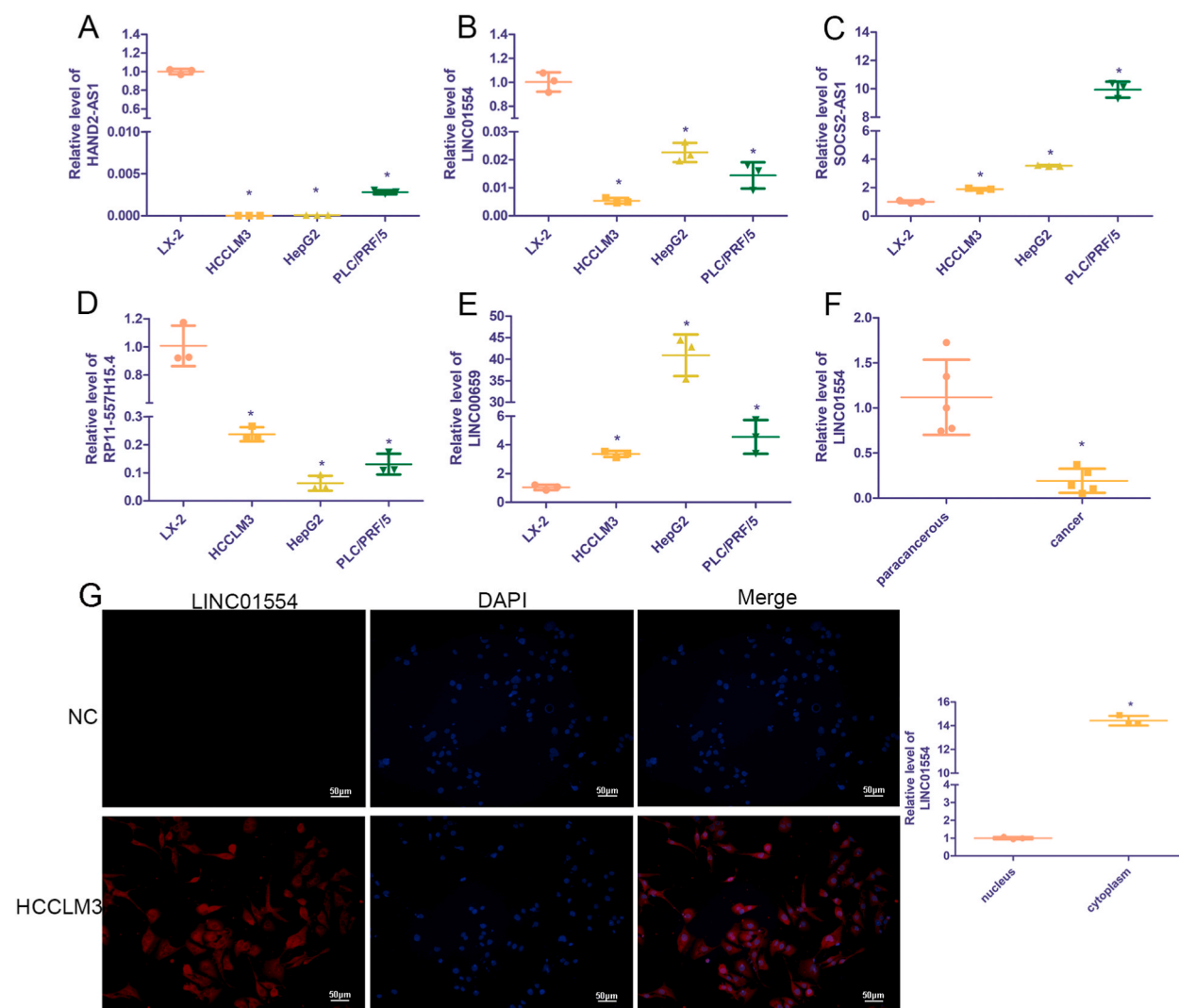


Fig. 1. Screen of the target lncRNA. Relative levels of HAND2-AS1 (A), LINC01554 (B), SOCS2-AS1 (C), RP11-557H15.4 (D) and LINC00659 (E) in the LX2 cells and liver cancer cell lines determined by real-time quantitative PCR (RT-qPCR). $N = 3$. Data were reported as mean \pm standard deviation (SD). *: $P < 0.05$, compared with the LX2 cells. (F) The relative level of LINC00659 in the cancer tissues and paraneoplastic tissues. $N = 5$. Data were reported as mean \pm SD. *: $P < 0.05$, compared with the paraneoplastic tissues. (G) The localization of lncRNA LINC01554 in HCCLM3 cells evaluated by fluorescence in situ hybridization. $N = 3$. Data were reported as mean \pm SD. *: $P < 0.05$, compared with the nucleus.

Bioengineering Co., Ltd., Wuhan, China). The protein samples (20 μ g) were separated by 10% SDS-PAGE, transferred to PVDF membranes, and then blocked with 5% skim milk at 37 °C for 2 h. After washing with PBST (1 mL Tween-20 in 1000 mL 1 \times PBS), the membranes were respectively incubated with anti-caspase3 antibody (1:1000, cat no. 19677-1-AP, Proteintech Group, Inc., Rosemont, IL, USA), anti-E-cadherin antibody (1:2000, cat no. 20874-1-AP, Proteintech Group, Inc.), anti-TIMP3 antibody (1:1000, cat no. 10858-1-AP, Proteintech Group, Inc.), and anti-GAPDH antibody (1:10000, cat no. 60004-1-AP, Proteintech Group, Inc.) overnight. The PVDF membrane was washed 3 times with TBST and incubated with the secondary antibody (goat anti-rabbit IgG-HRP, 1:5000, cat no. 111-035-003, Jackson ImmunoResearch, USA) at room temperature for 2 h. After washing 3 times with TBST, the protein-containing membrane was detected using the ECL chemiluminescence detection system (model no. T4600, Shanghai Tianneng Technology Co., Ltd., Shanghai, China).

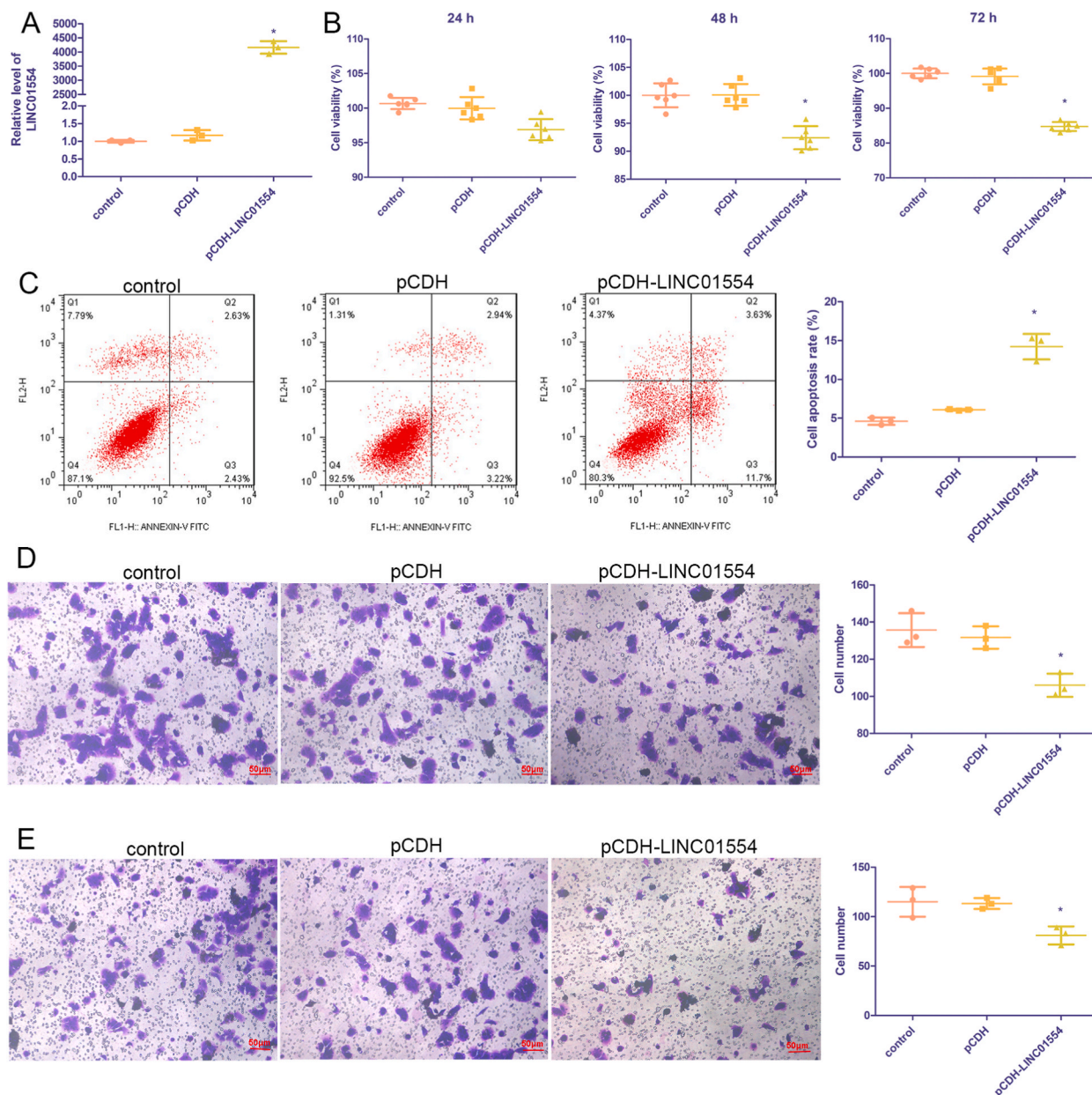


Fig. 2. The effects of LINC01554 on the cell function of HCCLM3 cells. (A) The relative level of LINC01554 after cell transfection measured by RT-qPCR. N = 3. (B) The cell viability of the HCCLM3 cells with LINC01554 overexpression using Cell Counting Kit-8 (CCK-8). N = 3. (C) The cell apoptosis of the HCCLM3 cells with LINC01554 overexpression determined by flow cytometer. N = 3. The cell migration (D) and invasion (E) of the HCCLM3 cells with LINC01554 overexpression measured by Transwell. N = 3. Data were reported as mean \pm SD. *: $P < 0.05$, compared with the control group.

2.10. Statistical analysis

Data were reported as mean \pm standard deviation (SD). All the statistical analyses were analyzed using Graphpad prism 5 (Graphpad Software, San Diego, CA). For the comparisons among more than two groups, one-way analysis of variance (ANOVA) and then Bonferroni test were applied. Student's T-test (two-tailed) was utilized to compare the difference between two groups. A value of $P < 0.05$ was considered as the significant difference.

3. Results

3.1. Screen of target lncRNA

Based on the previous study of He et al. [17], we randomly selected five down-regulated lncRNAs (HAND2-AS1, LINC01554, SOCS2-AS1, LINC00659 and RP11-557H15.4) in the liver cancer for further verification. It is clear that compared with the LX2 cells,

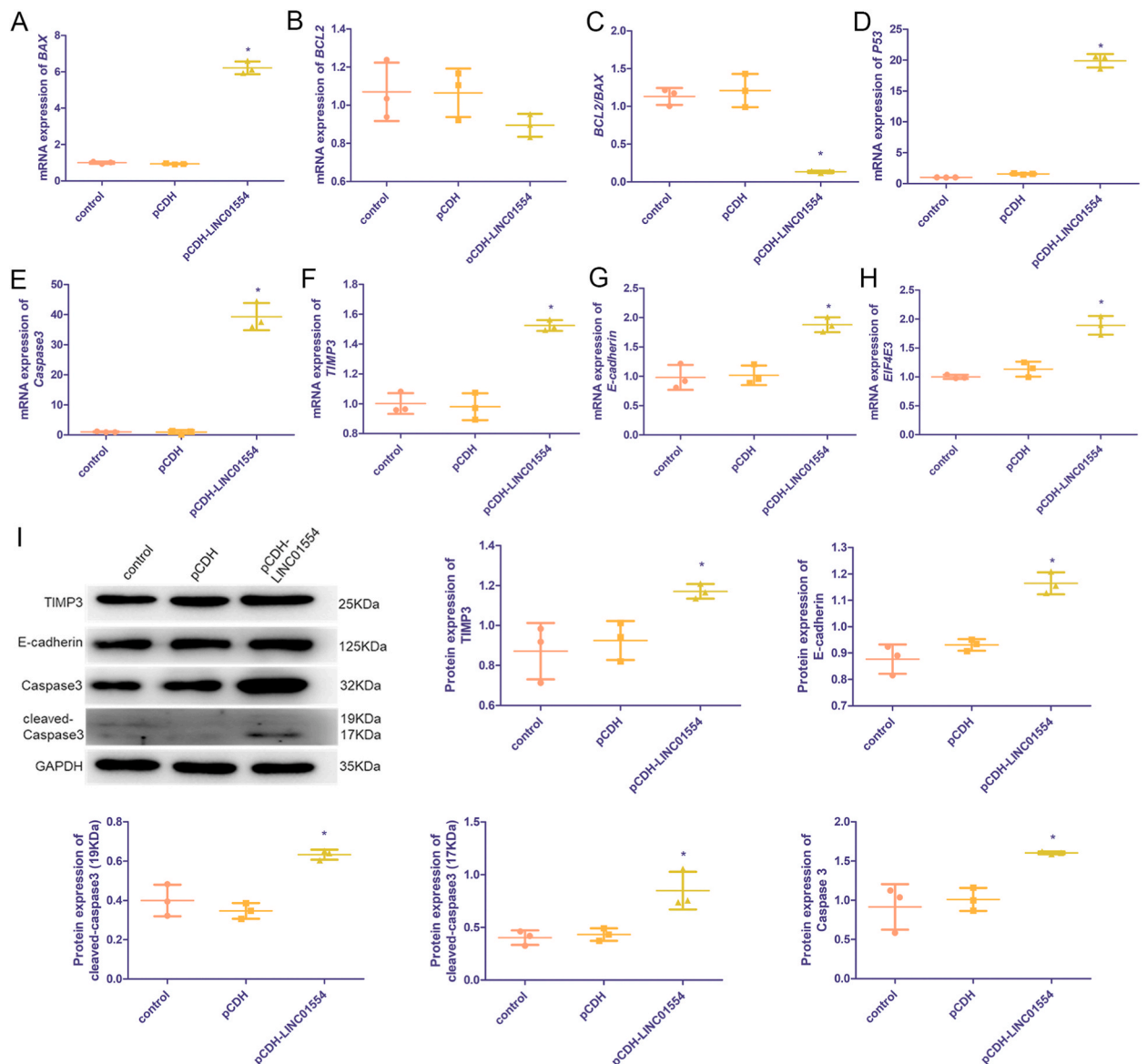


Fig. 3. The effects of LINC01554 on the expressions of related genes and proteins. The expression levels of BAX (A), BCL2 (B), BCL2/BAX (C), P53 (D), Caspase3 (E), TIMP3 (F), E-cadherin (G), EIF4E3 (H) after the cells transfected with pCDH-LINC01554. N = 3. (I) The representative images of protein bands measured by Western blot, and quantitative analysis. N = 3. Data were reported as mean \pm SD. *: $P < 0.05$, compared with the control group.

the relative levels of HAND2-AS1 and LINC01554 were significantly decreased in the HCCLM3, HepG2 and PLC/PRF/5 cell lines ($P < 0.05$, Fig. 1A and B). However, the relative levels of SOCS2-AS1 and LINC00659 were evidently higher in the liver cancer cell lines than those in the LX2 cells ($P < 0.05$, Fig. 1C–E). For RP11-557H15.4, its level was also significantly lower in the HCCLM3, HepG2 and PLC/PRF/5 cell lines than that in the LX2 cells ($P < 0.05$, Fig. 1D). After searching the literatures, the roles of lncRNA HAND2-AS1 in liver cancer have been fully reported previously ([11,18]), while no studies have reported the specific roles of lncRNA RP11-557H15.4 in human diseases. Additionally, for lncRNA LINC01554, some studies have reported its roles in other cancers, such as NSCLC [19], laryngeal squamous cell carcinoma [20], and esophageal squamous cell carcinoma [21], but its action mechanisms in HCC are still unclear. Additionally, it was also found that compared with the paracancerous tissues, the level of LINC01554 was significantly decreased in the cancer tissues ($P < 0.05$, Fig. 1F). The results of FISH found that LINC01554 was expressed in the cytoplasm of HCCLM3 cells, and the LINC01554 level in cytoplasm was significantly higher than that in the nucleus ($P < 0.05$, Fig. 1G). Therefore, we chose LINC01554 as the target for subsequent experiments.

3.2. LINC01554 overexpression inhibited viability, migration, and invasion, as well as promoted apoptosis of HCCLM3 cells

Firstly, HCCLM3 cells with LINC01554 overexpression were constructed, and the level of LINC01554 was detected by RT-qPCR. It is obvious that there was no significant difference in LINC01554 level between the control and pCDH groups ($P > 0.05$, Fig. 2A). Besides,

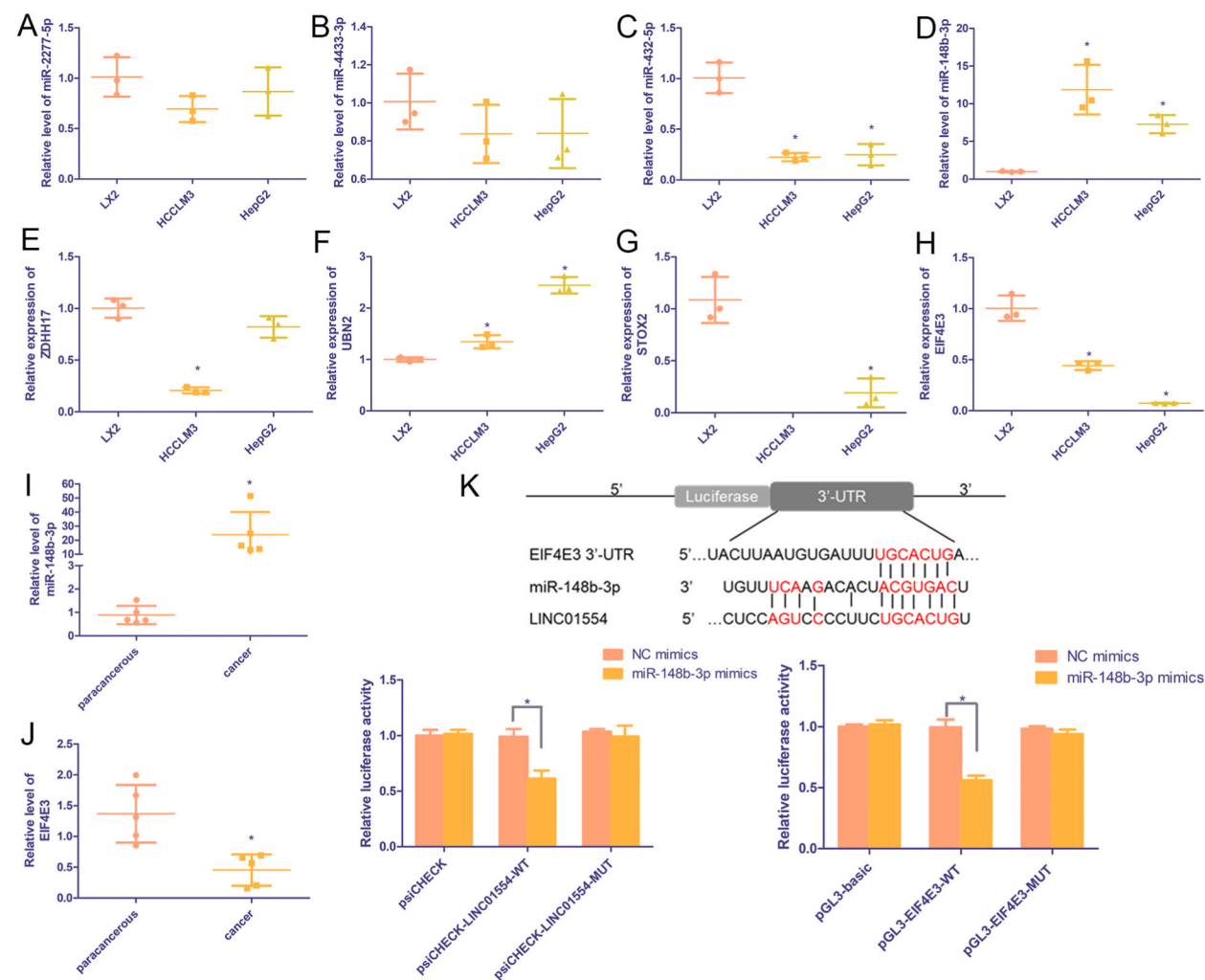


Fig. 4. LINC01554 interacted with miR-148b-3p and EIF4E3 each other. The relative levels of miR-2277-5p (A), miR-4433-3p (B), miR-432-5p (C) and miR-148b-3p (D) in the LX cells, HCCLM3 cells and HepG2 cells. $N = 3$. The relative expressions of ZDHH17 (E), UBN2 (F), STOX2 (G) and EIF4E3 (H) in the LX cells, HCCLM3 cells and HepG2 cells. $N = 3$. Data were reported as mean \pm SD. *: $P < 0.05$, compared with the LX2 cells. The relative level of miR-148b-3p (I) and EIF4E3 (J) in the cancer tissues and paracancerous tissues. $N = 5$. Data were reported as mean \pm SD. *: $P < 0.05$, compared with the paracancerous tissues. (K) The relative luciferase activity measured after 293T cells co-transferred with miR-148b-3p mimics or NC mimics and psiCHECK vector or psiCHECK-LINC01554-WT vector or psiCHECK-LINC01554-MUT vector. $N = 3$. Data were reported as mean \pm SD. *: $P < 0.05$.

the level of LINC01554 in the pCDH-LINC01554 group was about 4000 times greater than that in the control group (Fig. 2A), which indicated that the cells with LINC01554 overexpression were successfully established.

The effects of LINC01554 on the cell viability, apoptosis, migration, and invasion of HCCLM3 cells were then determined. All the results showed that no significant differences in the cell viability, apoptosis, migration, and invasion were found between control and pCDH groups ($P > 0.05$, Fig. 2B–E). After cultured for 24 h, no significant difference in the cell viability was also found in the control and pCDH-LINC01554 groups. However, after cultured for 48 h and 72 h, the cell viability in the pCDH-LINC01554 group was significantly decreased compared to the control group ($P < 0.05$, Fig. 2B). For cell apoptosis, the cell apoptosis rates in the control, pCDH and pCDH-LINC01554 groups were $4.61 \pm 0.46\%$, $6.07 \pm 0.10\%$, and $14.22 \pm 1.64\%$, respectively. These results showed that LINC01554 overexpression significantly promoted cell apoptosis of HCCLM3 cells compared with the control group ($P < 0.05$, Fig. 2C). For cell migration and invasion, their cell numbers in the pCDH-LINC01554 group were evidently lower than those in the control group ($P < 0.05$, Fig. 2D and E).

BAX, *BCL2*, *p53* and *Caspase3* are the apoptosis-related genes, as well as *TIMP3* and *E-cadherin* are the epithelial-mesenchymal transformation (EMT)-related genes. *EIF4E3*, as a specific tumor suppressor, was found to bind atypically to m7G cap to inhibit carcinogenic transformation of cells [24]. Therefore, RT-qPCR and Western blot were used to determine the expressions of the related genes/proteins. For *BAX*, its expression in the pCDH-LINC01554 group was significantly higher than that in the control group ($P < 0.05$, Fig. 3A). There was no significant difference in the *BCL2* expression among the control, pCDH and pCDH-LINC01554 groups ($P > 0.05$, Fig. 3B). Additionally, the ratio of *BCL2/BAX* in the pCDH-LINC01554 group was markedly reduced compared to the control group ($P < 0.05$, Fig. 3C). Compared with the control group, the expressions of *P53* and *Caspase3* in the pCDH-LINC01554 group showed an extremely significant increase ($P < 0.05$, Fig. 3D and E). For *TIMP3*, *E-cadherin* and *EIF4E3*, their expression was significantly up-regulated after LINC01554 overexpressed compared to the control cells ($P < 0.05$, Fig. 3F–H). Furthermore, Western blot was applied to examine the expressions of caspase 3, cleaved-Caspase3, *TIMP3* and *E-cadherin*. It is clear that the trend of caspase 3, cleaved-Caspase3, *TIMP3* and *E-cadherin* expressions measured by Western blot was similar with those determined by RT-qPCR (Fig. 3I, Fig. S1).

3.3. LINC01554 interacted with miR-148b-3p and EIF4E3

An online tool starbase (<http://starbase.sysu.edu.cn/index.php>) was used to predict the target miRNAs interacting with LINC01554. It was found that miR-2277-5p, miR-4433-3p, miR-432-5p and miR-148b-3p were the target miRNAs of LINC01554. Through RT-qPCR, no significant differences in the levels of miR-2277-5p and miR-4433-3p were found between LX2 cells and HCCLM3 cells ($P > 0.05$, Fig. 4A and B). The level of miR-432-5p was significantly lower in the HCCLM3 cells than that in the LX2 cells ($P < 0.05$, Fig. 4C). However, the level of miR-148b-3p in the HCCLM3 cells was significantly increased compared to the LX2 cells ($P < 0.05$, Fig. 4D), which was opposite to the trend of LINC01554 level.

Starbase (<http://starbase.sysu.edu.cn/index.php>) was also applied to predict the target mRNAs of miR-148b-3p, and then RT-qPCR was used to measure the expressions of these target mRNAs (*ZDHH17*, *UBN2*, *EIF43*, and *STOX2*). The expression of *ZDHH17* was significantly down-regulated in the HCCLM3 cells compared with the LX2 cells ($P < 0.05$); while showed no significant difference between LX2 cells and HepG2 cells ($P > 0.05$, Fig. 4E). For *UBN2*, its expression was evidently up-regulated in the HCCLM3 cells and HepG2 cells compared to the LX2 cells ($P < 0.05$, Fig. 4F). *STOX2* was not detected in the HCCLM3 cells, and was low expressed in the HepG2 cells, which suggested that *STOX2* was low abundance in the LX2 cells and liver cancer cells (Fig. 4G). Compared with the LX2 cells, the expression of *EIF4E3* in the liver cancer cells (HCCLM3 and HepG2) was significantly down-regulated ($P < 0.05$, Fig. 4H) which was opposite to the trend of miR-148b-3p level. Additionally, the expression levels of miR-148b-3p and *EIF4E3* were measured in the clinical tissue samples. It was found that compared with the paracancerous tissues, the level of miR-148b-3p was significantly increased in the cancer tissues ($P < 0.05$, Fig. 4I); while the *EIF4E3* expression was evidently down-regulated in the cancer tissues ($P < 0.05$, Fig. 4J). Therefore, miR-148b-3p and *EIF4E3* was selected for further experiments.

After that, dual-luciferase reporter gene assay was utilized to prove the relationship among LINC01554, miR-148b-3p and *EIF4E3* (Fig. 4K). As shown in Fig. 4K, there was no significant difference in relative luciferase activity among psiCHECK transfected with NC mimics and miR-148b-3p mimics, or psiCHECK-LINC01554-MUT transfected with NC mimics and miR-148b-3p mimics, and psiCHECK-LINC01554-WT transfected with NC mimics ($P > 0.05$). In the psiCHECK-LINC01554-WT, the relative luciferase activity was significantly decreased after transfected with miR-148b-3p mimics compared with that transfected with NC mimics ($P < 0.05$, Fig. 4K). For the relationship between miR-148b-3p and *EIF4E3*, the relative luciferase activity was evidently reduced in the pGL3-*EIF4E3*-WT transfected with miR-148b-3p mimics compared to the pGL3-*EIF4E3*-WT transfected with NC mimics ($P < 0.05$, Fig. 4K). All these results implied that LINC01554, miR-148b-3p and *EIF4E3* could interact with each other.

3.4. miR-148b-3p knockdown suppressed viability, migration, and invasion, while facilitated apoptosis of HCCLM3 cells

In order to evaluate the effects of miR-148b-3p on the cell function of HCCLM3 cells, the cells with miR-148b-3p knockdown were successfully established. After cultured for 24 h, no significant difference in the cell viability was found among the control, miRNA-NC and miR-148b-3p inhibitor groups ($P > 0.05$, Fig. 5A). After cultured for 48 h and 72 h, cell viability in the cells with miR-148b-3p knockdown was significantly decreased compared with the control cells ($P < 0.05$, Fig. 5A). Compared with the control cells, miR-148b-3p knockdown significantly increased the cell apoptosis rate ($P < 0.05$, Fig. 5B), and evidently reduced the cell number ($P < 0.05$, Fig. 5C and D). These results indicated that miR-148b-3p knockdown could inhibit cell viability, migration, and invasion of HCCLM3 cells, and promote their apoptosis.

RT-qPCR results showed that there were no significant differences in the levels of *BAX*, *BCL2*, *BCL2/BAX*, *P53*, *Caspase3*, *TIMP3*, *E-cadherin*, and *EIF4E3* between the control and miRNA NC groups ($P > 0.05$, Fig. 6A–H). Compared with the control cells, the expressions of *BAX* and *BCL2* in the cells with miR-148b-3p knockdown was significantly up-regulated ($P < 0.05$, Fig. 6A and B); while the level of *BCL2/BAX* was evidently reduced after miR-148b-3p knockdown ($P < 0.05$, Fig. 6C). The tendency of *P53* and *Caspase3* expressions in the different groups was similar with that of *BAX* expression (Fig. 6D and E). For *TIMP3*, *E-cadherin* and *EIF4E3*, their expressions were significantly higher in the cells with miR-148b-3p knockdown than those in the control cells ($P < 0.05$, Fig. 6F–H).

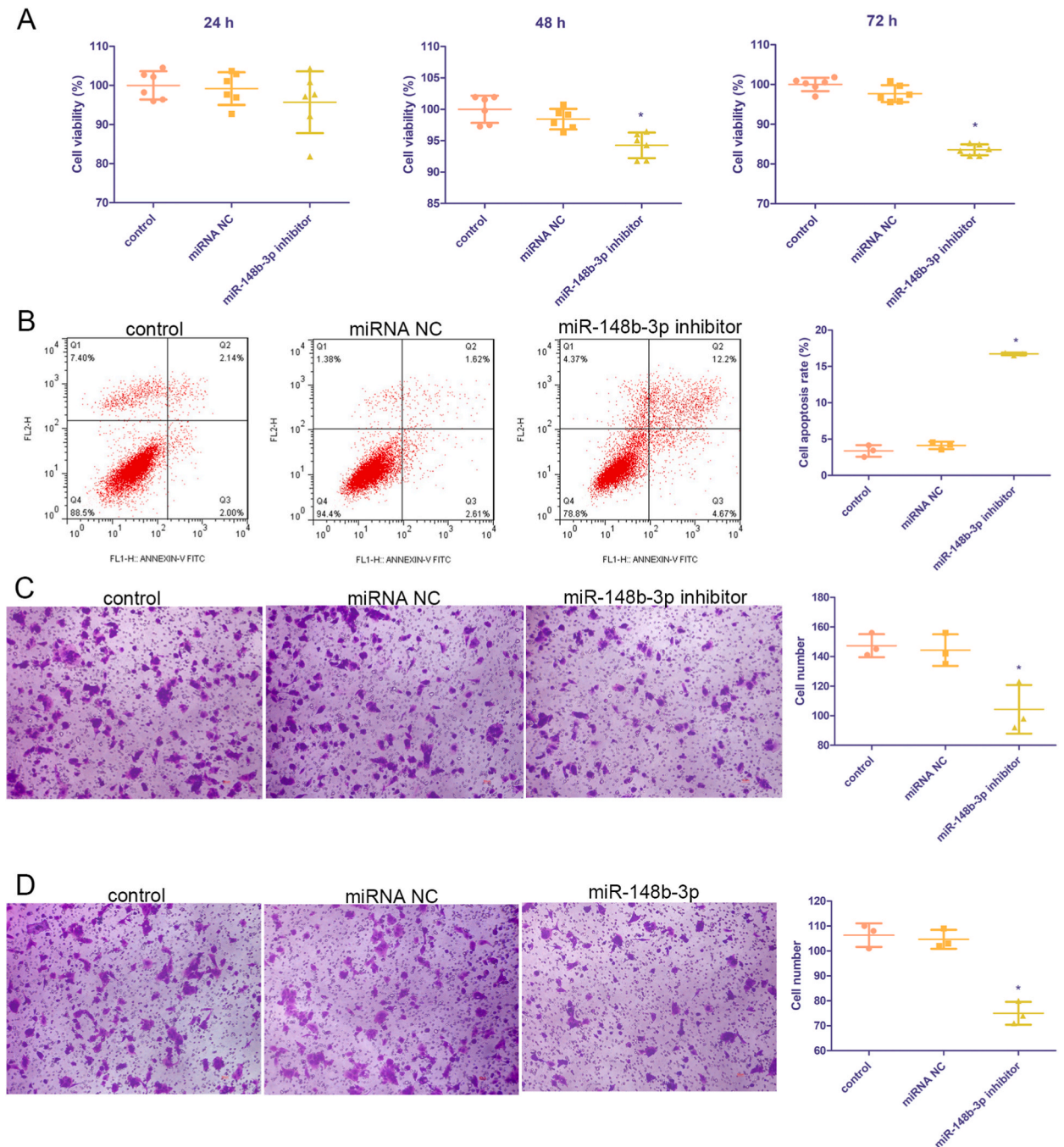


Fig. 5. The effects of miR-148b-3p on the cell function of HCCLM3 cells. (A) The cell viability of the HCCLM3 cells with miR-148b-3p knockdown using CCK-8. N = 3. (B) The cell apoptosis of the HCCLM3 cells with miR-148b-3p knockdown examined by flow cytometer. N = 3. The cell migration (C) and invasion (D) of the HCCLM3 cells with miR-148b-3p knockdown determined by Transwell. N = 3. Data were reported as mean ± SD. *: $P < 0.05$, compared with the control group.

Afterwards, Western blot was further to verify the expressions of cleaved-Caspase3, TIMP3 and E-cadherin. It was found that the tendency of Caspase 3, cleaved-Caspase3, TIMP3 and E-cadherin expressions detected by Western blot was similar with these examined by RT-qPCR (Fig. 6I, Fig. S2).

3.5. LINC01554 regulated cell function of HCCLM3 cells through miR-148b-3p/EIF4E3

No significant difference in the cell viability of HCCLM3 cells was found among the control, LINC01554-OE, and LINC01554-OE + miR-148b-3p-OE groups after 24 h of incubation ($P > 0.05$, Fig. 7A). However, after cultured for 48 h, and 72 h, LINC01554 over-expression significantly inhibited the cell viability of HCCLM3 cells compared with the control group ($P < 0.05$, Fig. 7A). However, when the cells were cultured for 48 h and 72 h, the cell viability in the LINC01554-OE + miR-148b-3p-OE group were significantly

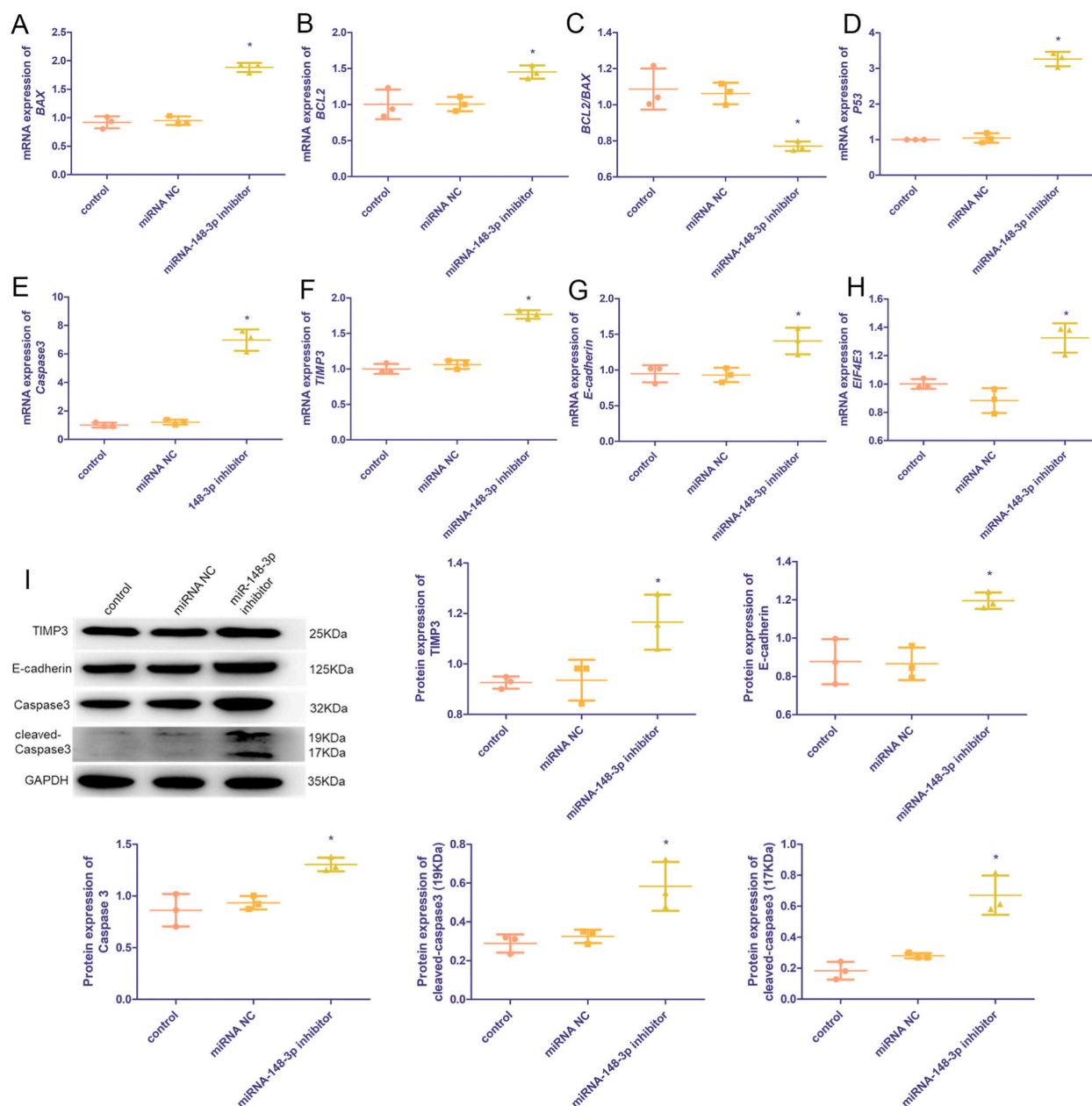


Fig. 6. The effects of miR-148b-3p on the expressions of related genes and proteins. The expression levels of BAX (A), BCL2 (B), BCL2/BAX (C), P53 (D), Caspase3 (E), TIMP3 (F), E-cadherin (G), EIF4E3 (H) after the cells transfected with miR-148b-3p inhibitor. N = 3. (I) The representative images of protein bands measured by Western blot, and quantitative analysis. N = 3. Data were reported as mean \pm SD. *: $P < 0.05$, compared with the control group.

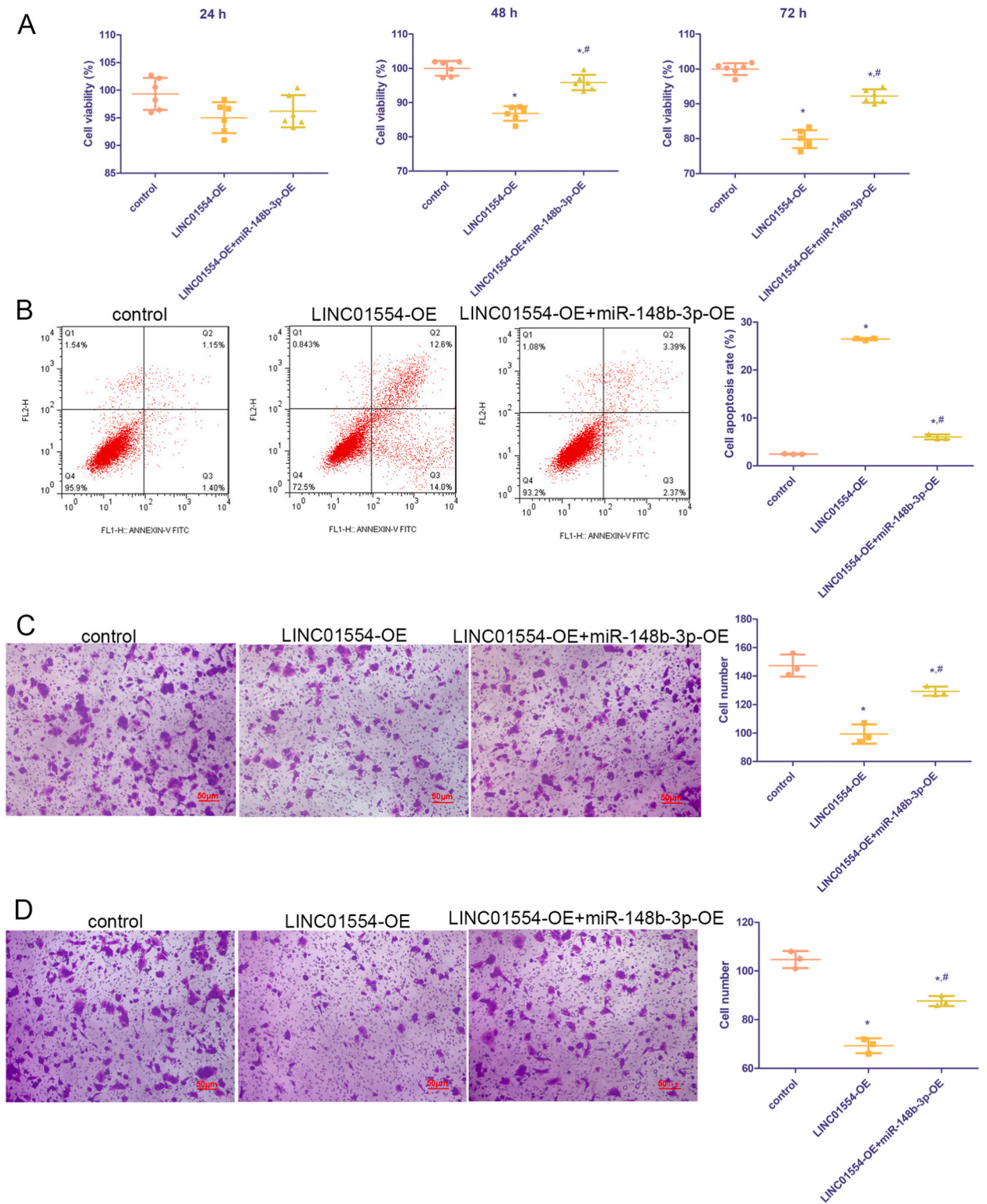


Fig. 7. LINC01554 regulated cell function of HCCLM3 cells via miR-148b-3p/EIF4E3. (A) The cell viability in different groups using CCK-8. N = 3. (B) The cell apoptosis in different groups by flow cytometer. N = 3. The cell migration (C) and invasion (D) in different groups detected by Transwell. N = 3. Data were reported as mean ± SD. *: $P < 0.05$, compared with the control group. #: $P < 0.05$, compared with the LINC01554-OE group.

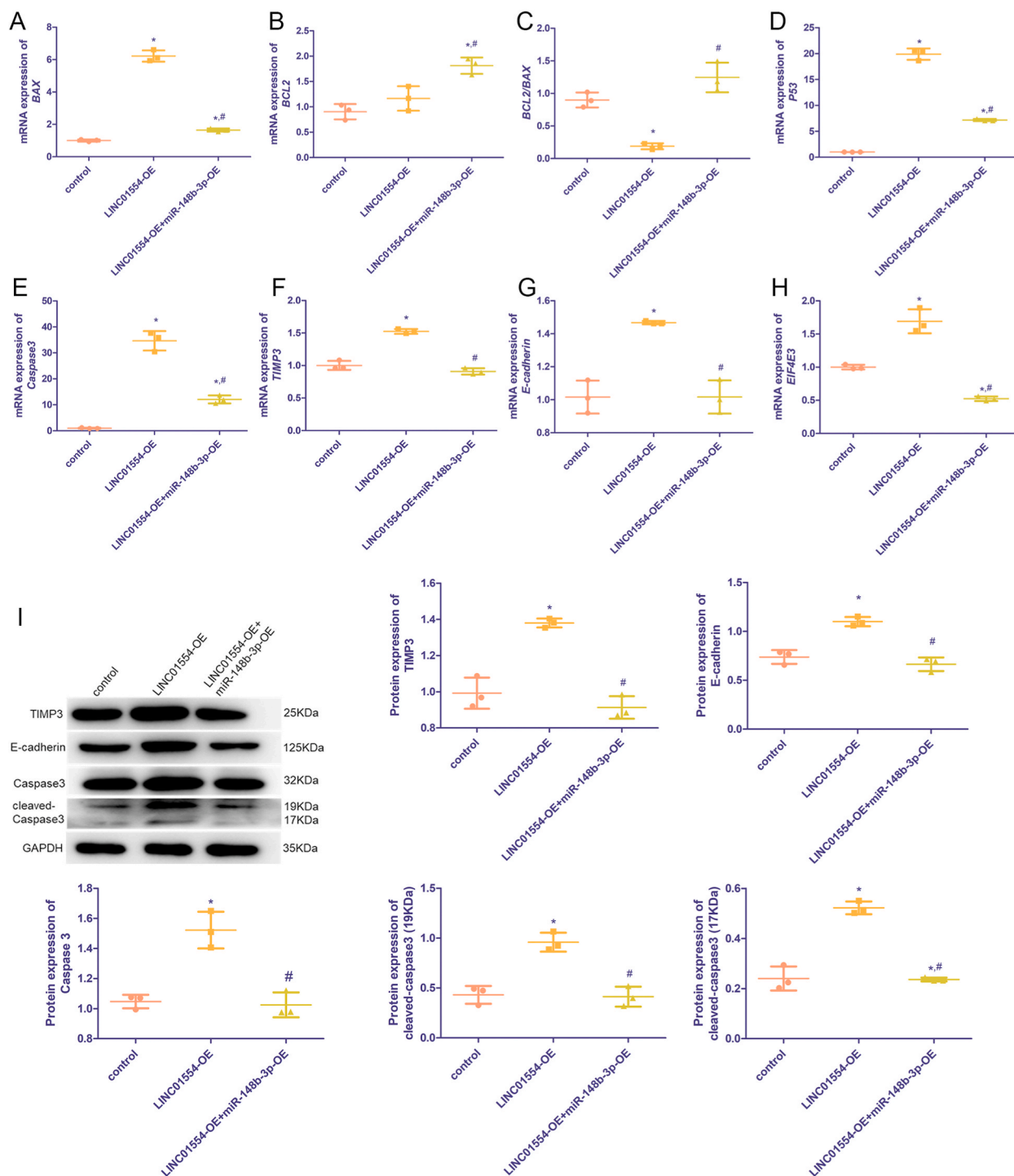


Fig. 8. The co-effects of LINC01554 and miR-148b-3p on the expressions of related genes and proteins. The expression levels of *BAX* (A), *BCL2* (B), *BCL2/BAX* (C), *P53* (D), *Caspase3* (E), *TIMP3* (F), *E-cadherin* (G), *EIF4E3* (H) in different groups. N = 3. (I) The representative images of protein bands measured by Western blot, and quantitative analysis. N = 3. Data were reported as mean ± SD. *: P < 0.05, compared with the control group. #: P < 0.05, compared with the LINC01554-OE group.

increased compared with the LINC01554-OE group ($P < 0.05$, Fig. 7A). Compared with the control group, LINC01554 overexpression significantly increased the cell apoptosis rate ($P < 0.05$); while after transfected with pCDH-LINC01554 and miR-148b-3p mimics together, the cell apoptosis rate was evidently reduced compared with the cells with LINC01554 overexpression ($P < 0.05$, Fig. 7B). Furthermore, the migration and invasion results showed that LINC01554 overexpression significantly decreased the cell number of HCCLM3 ($P < 0.05$), and miR-148b-3p mimics markedly increased the cell number induced by LINC01554 overexpression ($P < 0.05$, Fig. 7C and D).

Subsequently, the expression levels of BAX, BCL2, P53, Caspase3, TIMP3, E-cadherin, and EIF4E3 were determined by RT-qPCR and Western blot. Compared with the control group, LINC01554 overexpression significantly up-regulated the expressions of BAX, P53, Caspase3, TIMP3, E-cadherin and EIF4E3 ($P < 0.05$, Fig. 8A, D-H). When the cells were transfected with pCDH-LINC01554 and miR-148b-3p mimics together, the expression levels of BAX, P53, Caspase3, TIMP3, E-cadherin, and EIF4E3 induced by LINC01554 overexpression were significantly restored by miR-148b-3p mimics. For BCL2, its expression in the cells transfected with pCDH-LINC01554 and miR-148b-3p mimics together was significantly higher than that in the control cells and the cells with LINC01554 overexpression ($P < 0.05$, Fig. 8B). The level of BCL2/BAX was significantly decreased in the cells with LINC01554 overexpression compared with the control cells ($P < 0.05$); while miR-148b-3p mimics could restore its level to a similar level of the control group ($P > 0.05$, Fig. 8C). Additionally, it was found that the tendency of Caspase3, cleaved-caspase 3, TIMP3, and E-cadherin levels in different groups measured by Western blot were similar with that detected by RT-qPCR (Fig. 8I, Fig. 8J).

4. Discussion

Liver cancer is the most frequent fatal malignancy worldwide, seriously affecting people's health and life. Recently, more and more studies have found the important roles of lncRNAs in cancers. Our previous study has identified the DE-lncRNAs between liver cancer patients and healthy controls through lncRNA microarray [17]; however, the specific role of the lncRNAs in liver cancer and their related mechanisms remain unknown. In this study, LINC01554 was significantly down-regulated in the liver cancer cell lines, and was chosen as the subject lncRNA. It was also found that LINC01554 overexpression could inhibit viability, migration and invasion of HCCLM3 cells, and promote their apoptosis through regulating apoptosis-related genes, TIMP3, E-cadherin and EIF4E3. After that, miR-148b-3p and EIF4E3 were proved to be the interactive genes of LINC01554. The effects of miR-148b-3p knockdown on HCCLM3 cells were similar with those of LINC01554 overexpression. Finally, LINC01554 was verified at the cellular level to regulate the growth of HCC cells through miR-148b-3p/EIF4E3 axis. These results suggested that LINC01554/miR-148b-3p/EIF4E3 may be potential targets and a novel pathway for liver cancer therapy.

Previous studies have indicated that lncRNAs, as key regulators of tumor pathogenesis, are involved in multistep biological processes of various diseases and multilevel regulation of cancer gene expression ([25,26]). Our study found that LINC01554 was significantly down-regulated in the liver cancer cell lines compared with control liver cells, as well as LINC01554 overexpression significantly suppressed viability, migration, and invasion of HCCLM3 cells, and facilitated their apoptosis. Li et al. [27] reported that low level of LINC01554 was closely associated with overall survival, tumor size and pathological stage of HCC, and may be a therapeutic target for HCC. Another study demonstrated that lncRNA MEG3 was highly expressed in the para-carcinoma tissues compared to GC tissues, and overexpression of lncRNA MEG3 could control the proliferation and metastasis of GC by p53 signaling pathway [28]. Therefore, we speculated that LINC01554 overexpression may have protective effects on liver cancer through inhibiting the growth, migration, and invasion of liver cancer cells.

Further to investigate the molecular mechanisms of LINC01554 affecting the growth of HCCLM3 cells, RT-qPCR and Western blot were used to determine the expressions of related genes and proteins. It is clear that LINC01554 overexpression significantly up-regulated the levels of BAX, BCL2/BAX, P53, cleaved-Caspase3, TIMP3, E-cadherin and EIF4E3. BAX is a pro-apoptotic gene, and BCL2 is an anti-apoptotic gene. BAX and BCL2 both belong to BCL2 protein family, and their ratio decides the degree of cell apoptosis [29]. The increased level of BCL2/BAX ratio reflects the inhibition of cell apoptosis, otherwise, it reflects the enhancement of cell apoptosis [30]. Kleczka et al. showed that dysregulation of BCL2/BAX balance induced cell apoptosis of OV7 cells, and the expression of BAX was 10 times larger than that of BCL2 [31]. P53 and Caspase3 were the other apoptosis-related genes. P53, one of the most important tumor suppressor genes, plays an anticancer role through activating cell death, including inducing apoptosis and autophagy, as well as cell cycle arrest in cancer cells [32]. Caspase3, a key executor of cell apoptosis, can cleave many other critical functional proteins in cells after activated by Caspase8/9, thus leading to cell apoptosis [33]. A previous study of Weng et al. showed that silencing UBE4B induced apoptosis of nasopharyngeal carcinoma cells via up-regulating P53 and cleaved Caspase3 [34]. TIMP3, a secreted glycoprotein, plays an important role in carcinogenesis and protects the extracellular matrix from degradation [35]. Su et al. [36] demonstrated that overexpression of TIMP3 decreased the migration and invasion ability of oral cancer cells, and inhibited lymph node metastasis *in vivo*. E-cadherin is a transmembrane glycoprotein, and its loss contributes to EMT, which is the root cause of invasion and metastatic cancer cells spreading [37]. Niu et al. [38] indicated that miR-221-5p could promote the invasion and migration of breast cancer cells through regulating E-cadherin expression. Besides, EIF4E3 has been reported to be a new actor in mRNA metabolism and tumor suppressor [39]. Combined with our results, it can be inferred that LINC01554 overexpression may restrain the growth of liver cancer cells via regulating the apoptosis-related genes, EMT-related genes, and EIF4E3.

In addition, more and more studies have emphasized that lncRNAs located in different subcellular locations can participate in intracellular biological processes through different mechanisms [40]. The lncRNA in the cytoplasm activates/inhibits the intracellular signaling pathway by competing with the mRNA to bind to the miRNA [41]. Emerging evidences support the ceRNA hypothesis that the regulation of ceRNAs is involved in the carcinogenic effects of liver cancer ([42,43]). Therefore, FISH were used to determine the localization of LINC01554 in HCCLM3 cells, and it was found that LINC01554 was expressed in the cytoplasm of HCCLM3 cells. After

that, through bioinformatics analysis and dual luciferase reporter gene assay, we proved that LINC01554, miR-148b-3p and EIF4E3 could interact with each other. MiRNAs are small single-stranded non-coding RNAs composed of 18–22 nucleotides that regulate gene expression by interacting with the 3' UTR of target genes [44]. MiR-148b-3p belongs to miR-148/152 family, and has been reported to participate in many biological functions, including the growth, proliferation, invasion, and apoptosis of tumors [45]. However, the roles of miR-148b-3p in liver cancer are still unclear. This study elaborated that miR-148b-3p knockdown significantly inhibit the growth and invasion of liver cancer cells, and up-regulated pro-apoptotic genes, *TIMP3*, *E-cadherin* and *EIF4E3*. A recent study has shown that hypoxia induces the up-regulation of miR-148b-3p expression in lung adenocarcinoma cells, which in turn affects the tumor cell cycle by regulating *NOG* and *Wnt10b* [46]. Aure et al. integrated breast cancer copy number and methylation changes, and found that increased copy number and up-regulation of miR-148b-3p expression coexisted to promote tumor cell proliferation [47]. These findings together with our results supported that miR-148b-3p could influence the growth of liver cancer cells through regulating *EIF4E3*.

Further to confirm the relationship among LINC01554, miR-148b-3p and EIF4E3, pCDH-LINC01554 and miR-148b-3p mimics were transfected to HCCLM3 cells. It was found that miR-148b-3p mimics could reverse the changes of cell viability, apoptosis, migration and invasion induced by LINC01554 overexpression in HCCLM3 cells. A previous study of Zhang et al. [48] has displayed that overexpression of lncRNA MT1JP *in vivo* or *in vitro* inhibits GC cell proliferation, migration, invasion and promotes apoptosis by reducing miR-92a and promoting FBXW7, which indicated that lncRNA MT1JP could modulate GC progression by sponging miR-92a-3p to regulate FBXW7. Therefore, we can speculate that LINC01554 may affect growth, migration, and invasion of liver cancer cells through regulating miR-148b-3p/EIF4E3.

However, there are some limitations in this study. Firstly, the correlations among LINC01554, miR-148b-3p and EIF4E3 need to be further confirmed by rescue experiments, and more cell lines need to be used to investigate their effects on the growth and metastasis of liver cancer. Second, the levels of LINC01554 and miR-148b-3p in blood samples from liver cancer patients and normal healthy controls should be determined, and compared. Additionally, our findings need to be further verified *in vivo*, as well as the roles of the up-regulated lncRNAs in liver cancer should be explored in the future.

In conclusion, LINC01554 overexpression could suppress the growth and metastasis of HCCLM3 cells via regulating the expression of *EIF4E3*, the apoptosis-related genes, and EMT-related genes. The effects of miR-148b-3p knockdown on HCCLM3 cells were similar with those of LINC01554 overexpression. Besides, LINC01554, miR-148b-3p and EIF4E3 could interact with each other, and miR-148b-3p mimics could reverse the changes of cell functions induced by LINC01554 overexpression. Our findings will help us to improve our understanding of the occurrence and progression of liver cancer, and provide a basis for LINC01554/miR-148b-3p/EIF4E3 as novel therapeutic targets and pathways for the therapy of liver cancer.

5. Ethics approval and consent to participate

This study was approved by the Ethic Committee of Shanxi Bethune Hospital (Shanxi, China) (approval no. YXLL-2022-005); and written informed consent was obtained from all patients.

Funding

The present study was funded by grants from the Research Project Supported by Shanxi Scholarship Council of China (grant nos. 2021-166), Human Resources and Social Security Department System of Shanxi Province (Grant No. 20210001), Shanxi '136' Leading Clinical Key Specialty (Grant No. 2019XY002), and Shanxi Provincial Key Laboratory of Hepatobiliary and Pancreatic Diseases (under construction).

Data availability

The dataset used and/or analyzed during the current study are available from the corresponding author on reasonable request.

CRedit authorship contribution statement

Xiaojing Ren: Writing – original draft, Methodology, Investigation, Formal analysis, Conceptualization. **Xiaoxiao Wang:** Methodology, Investigation, Formal analysis, Data curation. **Huangqin Song:** Software, Resources, Methodology, Investigation. **Chao Zhang:** Validation, Software, Methodology, Formal analysis. **Junlong Yuan:** Validation, Software, Resources, Methodology. **Jiefeng He:** Writing – review & editing, Supervision, Project administration, Funding acquisition, Conceptualization. **Jianguo Li:** Writing – review & editing, Validation, Supervision, Funding acquisition, Conceptualization. **Zhuangqiang Wang:** Writing – review & editing, Visualization, Supervision, Funding acquisition, Conceptualization.

Declaration of competing interest

The authors declare that they have no known competing financial interests or personal relationships that could have appeared to influence the work reported in this paper.

Acknowledgement

Not applicable.

Appendix A. Supplementary data

Supplementary data to this article can be found online at <https://doi.org/10.1016/j.heliyon.2024.e27319>.

References

- [1] H. Sung, J. Ferlay, R.L. Siegel, M. Laversanne, I. Soerjomataram, A. Jemal, F. Bray, Global cancer statistics 2020: GLOBOCAN estimates of incidence and mortality worldwide for 36 cancers in 185 countries, *CA A Cancer J. Clin.* 71 (2021) 209–249.
- [2] W. Cao, H.D. Chen, Y.W. Yu, N. Li, W.Q. Chen, Changing profiles of cancer burden worldwide and in China: a secondary analysis of the global cancer statistics 2020, *Chin. Med. J.* 134 (2021) 783–791.
- [3] L. Lin, L. Yan, Y. Liu, C. Qu, J. Ni, H. Li, The burden and trends of primary liver cancer caused by specific etiologies from 1990 to 2017 at the global, regional, national, age, and sex level results from the global burden of disease study 2017, *Liver Cancer* 9 (2020) 563–582.
- [4] M.M. Center, A. Jemal, International trends in liver cancer incidence rates, *Cancer Epidemiol. Biomarkers Prev.* 20 (2011) 2362–2368.
- [5] D. Anwanwan, S.K. Singh, S. Singh, V. Saikam, R. Singh, Challenges in liver cancer and possible treatment approaches, *Biochim. Biophys. Acta Rev. Canc* 1873 (2020) 188314.
- [6] A.G. Singal, H.B. El-Serag, Hepatocellular carcinoma from epidemiology to prevention: translating knowledge into practice, *Clin. Gastroenterol. Hepatol.* 13 (2015) 2140–2151.
- [7] Y. Huang, The novel regulatory role of lncRNA-miRNA-mRNA axis in cardiovascular diseases, *J. Cell Mol. Med.* 22 (2018) 5768–5775.
- [8] W.X. Peng, P. Koirala, Y.Y. Mo, LncRNA-mediated regulation of cell signaling in cancer, *Oncogene* 36 (2017) 5661–5667.
- [9] A. Bhan, M. Soleimani, S.S. Mandal, Long noncoding RNA and cancer: a new paradigm, *Cancer Res.* 77 (2017) 3965–3981.
- [10] K. Yuan, J. Lan, L. Xu, et al., Long noncoding RNA TLNC1 promotes the growth and metastasis of liver cancer via inhibition of p53 signaling, *Mol. Cancer* 21 (2022) 105.
- [11] Y. Wang, P. Zhu, J. Luo, et al., LncRNA HAND2-AS1 promotes liver cancer stem cell self-renewal via BMP signaling, *EMBO J.* 38 (2019) e101110.
- [12] X. Xin, M. Wu, Q. Meng, et al., Long noncoding RNA HULC accelerates liver cancer by inhibiting PTEN via autophagy cooperation to miR15a, *Mol. Cancer* 17 (2018) 94.
- [13] R.S. Zhou, E.X. Zhang, Q.F. Sun, Z.J. Ye, J.W. Liu, D.H. Zhou, Y. Tang, Integrated analysis of lncRNA-miRNA-mRNA ceRNA network in squamous cell carcinoma of tongue, *BMC Cancer* 19 (2019) 779.
- [14] J. Jiang, Y. Bi, X.P. Liu, et al., To construct a ceRNA regulatory network as prognostic biomarkers for bladder cancer, *J. Cell Mol. Med.* 24 (2020) 5375–5386.
- [15] X.Z. Yang, T.T. Cheng, Q.J. He, et al., LINC01133 as ceRNA inhibits gastric cancer progression by sponging miR-106a-3p to regulate APC expression and the Wnt/beta-catenin pathway, *Mol. Cancer* 17 (2018) 126.
- [16] W. Zhao, D. Geng, S. Li, Z. Chen, M. Sun, LncRNA HOTAIR influences cell growth, migration, invasion, and apoptosis via the miR-20a-5p/HMGA2 axis in breast cancer, *Cancer Med.* 7 (2018) 842–855.
- [17] J. He, H. Zhao, D. Deng, Y. Wang, X. Zhang, H. Zhao, Z. Xu, Screening of significant biomarkers related with prognosis of liver cancer by lncRNA-associated ceRNAs analysis, *J. Cell. Physiol.* 235 (2020) 2464–2477.
- [18] D. Yan, F. Jin, Y. Lin, lncRNA HAND2-AS1 inhibits liver cancer cell proliferation and migration by upregulating SOCS5 to inactivate the JAK-STAT pathway, *Cancer Biother. Radiopharm.* 35 (2020) 143–152.
- [19] Z. Wang, B. Yang, J. Zhang, X. Chu, Long noncoding RNA LINC01554 inhibits the progression of NSCLC progression by functioning as a ceRNA for miR-1267 and regulating ING3/Akt/mTOR pathway, *BioMed Res. Int.* 2022 (2022) 7162623.
- [20] J. Wang, W. Meng, J. Yang, et al., Aberrant methylation-mediated downregulation of the LINC01554 gene accelerates the malignant progression and regulates the chemosensitivity of laryngeal squamous cell carcinoma, *J. Physiol. Pharmacol.* (2022) 73.
- [21] Y. Zheng, J. Wu, R. Deng, et al., G3BP2 regulated by the lncRNA LINC01554 facilitates esophageal squamous cell carcinoma metastasis through stabilizing HDGF transcript, *Oncogene* 41 (2022) 515–526.
- [22] G. Xu, R. Ao, Z. Zhi, J. Jia, B. Yu, miR-21 and miR-19b delivered by hMSC-derived EVs regulate the apoptosis and differentiation of neurons in patients with spinal cord injury, *J. Cell. Physiol.* 234 (2019) 10205–10217.
- [23] Y. Lin, Y. Jin, T. Xu, S. Zhou, M. Cui, MicroRNA-215 targets NOB1 and inhibits growth and invasion of epithelial ovarian cancer, *Am J Transl Res* 9 (2017) 466–477.
- [24] Y. Zhang, W. Gan, N. Ru, et al., Comprehensive multi-omics analysis reveals m7G-related signature for evaluating prognosis and immunotherapy efficacy in osteosarcoma, *J. Bone Oncol.* 40 (2023) 100481.
- [25] L.J. Lim, S.Y.S. Wong, F. Huang, et al., Roles and regulation of Long noncoding RNAs in hepatocellular carcinoma, *Cancer Res.* 79 (2019) 5131–5139.
- [26] C.P. Bracken, H.S. Scott, G.J. Goodall, A network-biology perspective of microRNA function and dysfunction in cancer, *Nat. Rev. Genet.* 17 (2016) 719–732.
- [27] L. Li, K. Huang, Z. Lu, H. Zhao, H. Li, Q. Ye, G. Peng, Bioinformatics analysis of LINC01554 and its coexpressed genes in hepatocellular carcinoma, *Oncol. Rep.* 44 (2020) 2185–2197.
- [28] G.H. Wei, X. Wang, lncRNA MEG3 inhibit proliferation and metastasis of gastric cancer via p53 signaling pathway, *Eur. Rev. Med. Pharmacol. Sci.* 21 (2017) 3850–3856.
- [29] P.P. Ruvolo, X. Deng, W.S. May, Phosphorylation of Bcl2 and regulation of apoptosis, *Leukemia* 15 (2001) 515–522.
- [30] K. Vucicevic, V. Jakovljevic, N. Colovic, et al., Association of bax expression and Bcl2/Bax ratio with clinical and molecular prognostic markers in chronic lymphocytic leukemia, *J. Med. Biochem.* 35 (2016) 150–157.
- [31] A. Kleczka, R. Kubina, R. Dzik, K. Jasik, J. Stojko, K. Cholewa, A. Kabala-Dzik, Caffeic acid phenethyl ester (CAPE) induced apoptosis in serous ovarian cancer OV7 cells by deregulation of BCL2/BAX genes, *Molecules* 25 (2020).
- [32] S.B. Lee, S. Lee, J.Y. Park, S.Y. Lee, H.S. Kim, Induction of p53-dependent apoptosis by prostaglandin A2, *Biomolecules* 10 (2020).
- [33] M. Zhou, X. Liu, Z. Li, Q. Huang, F. Li, C.Y. Li, Caspase-3 regulates the migration, invasion and metastasis of colon cancer cells, *Int. J. Cancer* 143 (2018) 921–930.
- [34] C. Weng, Y. Chen, Y. Wu, et al., Silencing UBE4B induces nasopharyngeal carcinoma apoptosis through the activation of caspase3 and p53, *OncoTargets Ther.* 12 (2019) 2553–2561.
- [35] C.W. Su, C.W. Lin, W.E. Yang, S.F. Yang, TIMP-3 as a therapeutic target for cancer, *Ther Adv Med Oncol* 11 (2019), 1758835919864247.
- [36] C.W. Su, Y.C. Chang, M.H. Chien, Y.H. Hsieh, M.K. Chen, C.W. Lin, S.F. Yang, Loss of TIMP3 by promoter methylation of Sp1 binding site promotes oral cancer metastasis, *Cell Death Dis.* 10 (2019) 793.
- [37] I.V. Bure, M.V. Nemtsova, D.V. Zaletaev, Roles of E-cadherin and noncoding RNAs in the epithelial-mesenchymal transition and progression in gastric cancer, *Int. J. Mol. Sci.* 20 (2019).

- [38] X.Y. Niu, Z.Q. Zhang, P.L. Ma, MiRNA-221-5p promotes breast cancer progression by regulating E-cadherin expression, *Eur. Rev. Med. Pharmacol. Sci.* 23 (2019) 6983–6990.
- [39] L. Volpon, M.J. Osborne, B. Culjkovic-Kraljacic, K.L. Borden, eIF4E3, a new actor in mRNA metabolism and tumor suppression, *Cell Cycle* 12 (2013) 1159–1160.
- [40] L.L. Chen, Linking Long noncoding RNA localization and function, *Trends Biochem. Sci.* 41 (2016) 761–772.
- [41] A.M. Schmitt, H.Y. Chang, Long noncoding RNAs in cancer pathways, *Cancer Cell* 29 (2016) 452–463.
- [42] H. Wang, X. Huo, X.R. Yang, et al., STAT3-mediated upregulation of lncRNA HOXD-AS1 as a ceRNA facilitates liver cancer metastasis by regulating SOX4, *Mol. Cancer* 16 (2017) 136.
- [43] D.L. Chen, Y.X. Lu, J.X. Zhang, et al., Long non-coding RNA UICLM promotes colorectal cancer liver metastasis by acting as a ceRNA for microRNA-215 to regulate ZEB2 expression, *Theranostics* 7 (2017) 4836–4849.
- [44] M. Yi, L. Xu, Y. Jiao, S. Luo, A. Li, K. Wu, The role of cancer-derived microRNAs in cancer immune escape, *J. Hematol. Oncol.* 13 (2020) 25.
- [45] Y. Chen, Y. Song, Z. Wang, Z. Yue, H. Xu, C. Xing, Z. Liu, Altered expression of MiR-148a and MiR-152 in gastrointestinal cancers and its clinical significance, *J. Gastrointest. Surg.* 14 (2010) 1170–1179.
- [46] Y. Geng, L. Deng, D. Su, J. Xiao, D. Ge, Y. Bao, H. Jing, Identification of crucial microRNAs and genes in hypoxia-induced human lung adenocarcinoma cells, *OncoTargets Ther.* 9 (2016) 4605–4616.
- [47] M.R. Aure, S.K. Leivonen, T. Fleischer, et al., Individual and combined effects of DNA methylation and copy number alterations on miRNA expression in breast tumors, *Genome Biol.* 14 (2013) R126.
- [48] G. Zhang, S. Li, J. Lu, et al., LncRNA MT1JP functions as a ceRNA in regulating FBXW7 through competitively binding to miR-92a-3p in gastric cancer, *Mol. Cancer* 17 (2018) 87.